
CONTRIBUTIONS OF EL NIÑO SOUTHERN OSCILLATION (ENSO) DIVERSITY TO LOW-FREQUENCY CHANGES IN ENSO VARIANCE

Jakob Schlör

Machine Learning in Climate Science
University of Tübingen, Germany
jakob.schloer@uni-tuebingen.de

Felix Strnad

Machine Learning in Climate Science
University of Tübingen, Germany

Antonietta Capotondi

Cooperative Institute for Research in Environmental Sciences
University of Colorado, Boulder, CO
NOAA/Physical Sciences Laboratory, Boulder, CO

Bedartha Goswami

Machine Learning in Climate Science
University of Tübingen, Germany

ABSTRACT

El Niño Southern Oscillation (ENSO) diversity is characterized based on the longitudinal location of maximum sea surface temperature anomalies (SSTA) and amplitude in the tropical Pacific, as Central Pacific (CP) events are typically weaker than Eastern Pacific (EP) events. SSTA pattern and intensity undergo low-frequency modulations, affecting ENSO prediction skill and remote impacts. Yet, how different ENSO types contribute to these decadal variations and long-term variance trends remain uncertain. Here, we decompose the low-frequency changes of ENSO variance into contributions from ENSO diversity categories. We propose a fuzzy clustering of monthly SSTA to allow for non-binary event category memberships. Our approach identifies two La Niña and three El Niño categories and shows that the shift of ENSO variance in the mid-1970s is associated with an increasing likelihood of strong La Niña and extreme El Niño events.

Keywords El Niño Southern Oscillation Diversity · Unsupervised fuzzy clustering · Decadal variability

1 Introduction

The El Niño-Southern Oscillation (ENSO), characterized by anomalous sea surface temperatures (SSTs) in the tropical Pacific, exhibits notable diversity in its amplitude, temporal evolution, and spatial pattern. The El Niño events of 1982-83 and 1997-98, for instance, recorded exceptionally high SST anomaly (SSTA) values in the eastern equatorial Pacific, whereas the El Niño of 2002-03 was less extreme and exhibited the largest anomalies in the central equatorial Pacific (McPhaden, 2004). In order to describe these event-to-event differences, El Niño events have been generally categorized as Eastern Pacific (EP), and Central Pacific (CP) types (Capotondi et al., 2015). EP El Niño events typically have their peak SSTA in the eastern Pacific, may exhibit stronger intensities, and a largely reduced zonal thermocline slope, resulting in the pronounced discharge of warm water from the equatorial thermocline. In contrast, CP events show peak SSTA in the central Pacific and are comparatively weaker with smaller changes in zonal thermocline slope and warm water discharge (Kug et al., 2009; Capotondi, 2013).

These different types of ENSO events have substantially different downstream impacts on the global climate (Strnad et al., 2022; Beniche, 2023). For example, extreme drought conditions were recorded in eastern Australia in 2002, while a minor impact on precipitation was detected during the extreme 1997 event (Wang and Hendon, 2007). Weaker and shorter-lived CP events are associated with warm conditions in the equatorial Atlantic during boreal winter, while stronger and persistent EP events lead to cold anomalies in that area, with different impacts on precipitation over northeastern Brazil (Kao and Yu, 2009; Rodrigues et al., 2011). Thus, a deeper understanding of ENSO diversity is critical to support predictions of ENSO impacts.

ENSO characteristics, including amplitude and spatial pattern, exhibit decadal variations, which are mediated by changes in the background state of the tropical Pacific (Capotondi et al., 2023). Notable decadal phase transitions were observed in the late 1970s (Miller et al., 1994) and around the year 2000 (McPhaden, 2012). Paleoclimate data also indicate an increase in ENSO amplitude over recent decades (Grothe et al., 2020), consistent with modeling results showing a significant increase in ENSO amplitude after 1960, which was attributed to anthropogenic forcing (Cai et al., 2023). Analysis of a large number of observationally-based datasets revealed that the longitudinal location of the maximum SST anomalies, as well as the intensity of both El Niño and La Niña events, undergo decadal fluctuations (Dieppois et al., 2021), which can, in turn, modulate ENSO predictions (Lou et al., 2023). However, event location and intensity were considered separately by Dieppois et al. (2021), so that the contribution of different ENSO types to these decadal changes and long-term trends in ENSO variance remains unclear. Paleoclimate data (Lawman et al., 2022) indicate that extreme ENSO events may contribute to increases in ENSO variance. Similarly, climate models that capture relevant aspects of ENSO nonlinearities project an increase in ENSO variance that is linked to an increase in the frequency of extreme ENSO events (Cai et al., 2021). However, a more comprehensive understanding of these changes from an ENSO diversity perspective is still missing.

One main reason hindering the estimation of the contribution of different ENSO categories to its decadal modulation is that ENSO classifications often depend on the chosen definitions (Pascolini-Campbell et al., 2015; Yu and Kim, 2013; Capotondi et al., 2020a; Abdelkader Di Carlo et al., 2023). The disagreement between different ENSO classification methods is likely due to the assumption that ENSO events can be classified into binary types, based on indices capturing the location of the highest SSTA in the Tropical Pacific (like the Niño3 and Niño4 regions), or using Empirical Orthogonal Functions (EOFs) (Ashok et al., 2007; Kug et al., 2009; Kao and Yu, 2009; Takahashi et al., 2011). However, ENSO events are continuously distributed in the space spanned by the two leading principal components (PCs) (Takahashi and Dewitte, 2016; Cai et al., 2018; Capotondi et al., 2020a). Approaches that use a more continuous distribution of SSTAs to identify diversity show that events occur over multiple locations but with enhanced probabilities over the central and eastern tropical Pacific (Dieppois et al., 2021; Shin et al., 2021). In addition, both EP- and CP-type events appear to share common underlying dynamical processes, albeit with varying relevance depending on the longitude (Capotondi, 2013).

A notable example of an El Niño that eludes a binary classification is the 2015/16 events. While its SSTA and several of its impacts were typical of extreme EP events (Santoso et al., 2017), this event was not associated with a significant impact on California precipitation and was not followed by a strong La Niña, as other events of this type (i.e., 1982-83 and 1997-98). Indeed, this event was considered a mixture of EP and CP types (Paek et al., 2017; Capotondi et al., 2020a).

Here, we propose a new approach for characterizing ENSO diversity to better understand its relationship with decadal changes in ENSO variance. To that end, we develop a fuzzy clustering of the low-dimensional representation of monthly SSTA in the PC1-PC2 space to achieve a non-binary event categorization (i.e., events belonging to one cluster or not). Instead, in this fuzzy clustering approach, individual events are assigned a probability of belonging to a given cluster. Such membership probabilities are then used to determine their relative contributions to the low-frequency ENSO variance.

2 Methodology and data

2.1 Data

Our analysis is conducted on monthly SSTA in the tropical Pacific (130°E-70°W, 30°S-30°N) from eight reanalysis datasets merged together (Tab. S1 and SI Sec. S1). To ensure the same number of data points per month, we randomly select four data points per month from the eight datasets covering 1901–2022. While the dimensionality reduction encompasses all months, we select El Niño and La Niña winter months for the fuzzy clustering. Boreal winters (December-January-February (DJF)) are selected as El Niño (La Niña) when the average SSTA in the Niño3.4 region is larger than 0.5 K (smaller than -0.5 K).

2.2 Fuzzy clustering

Clustering algorithms are typically based on a distance measure between data points which becomes ill-posed in high-dimensional spaces (Parsons et al., 2004). To mitigate this issue, we first reduce the dimensionality of the geospatial fields before applying fuzzy clustering using EOF analysis.

Our input data, $X = (x(t_1), \dots, x(t_N))$, which consists of tropical Pacific SSTA fields $x(t) \in \mathcal{R}^{\mathcal{N}_{\text{lon}} \cdot \mathcal{N}_{\text{lat}}}$, are projected onto the first two EOF patterns to obtain the two PCs $z(t) \in \mathcal{R}^{\mathcal{E}}$, referred to as a latent vector. Besides EOFs, we also

use a nonlinear dimensionality reduction method, specifically a convolutional autoencoder neural network (SI Sec. S2, Fig. S1).

We apply the Gaussian Mixture Model (GMM), a probabilistic unsupervised clustering approach to identify different types of ENSO events. GMMs describe each cluster via a multivariate Gaussian distribution, accommodating overlapping probabilities. Mathematically, GMMs assume that the probability distribution of latent states, $p(z)$, comprises a mixture of Gaussians:

$$p(z) = \sum_{k=1}^K \pi_k \mathcal{N}(z | \mu_k, \Sigma_k), \quad (1)$$

with K representing the number of Gaussians, $\mathcal{N}(z | \mu_k, \Sigma_k)$, each characterized by a mean μ_k and covariance Σ_k . The probability of each Gaussian is denoted as $p(c_k) = \pi_k$ with $\sum_{k=1}^K \pi_k = 1$. The optimal number of clusters K is obtained, by minimizing the Bayesian Information Criterion (BIC). The BIC balances model complexity and fit quality, as described by Schwarz (1978) and in SI Sec. S3.

2.3 Variability estimation

The GMM allows assigning a probability, $p(c_k|z(t))$, to each data point, $z(t)$, that quantifies its likelihood of belonging to category c_k . These are the category memberships of the data point (Sec. S4), which are inherently fuzzy and non-binary (i.e. they are probabilities between 0 and 1), and allow us to model ENSO events in terms of their likelihood of occurrence. As a consequence, we can decompose a variable $y(t)$, for instance, SSHA, into the contributions of each category, by

$$y(t) = \sum_k p(c_k|z(t)) \cdot y(t) := \sum_k y_k(t) \quad (2)$$

where $y_k(t)$ is defined as the contribution of category c_k . Averaging $y_k(t)$ over time corresponds to a weighted average, with the weights being the categorical memberships (Sec. S5). Similarly, we can write the variance $\langle y^2 \rangle$, as

$$\langle y^2 \rangle = \left\langle \left(\sum_k y_k \right)^2 \right\rangle = \sum_k \langle y_k^2 \rangle + \sum_{l \neq m} \langle y_l y_m \rangle, \quad (3)$$

where $\langle y_k^2 \rangle$ is the variance contribution of category c_k and $\langle y_l y_m \rangle$ is the co-variability of categories l and m .

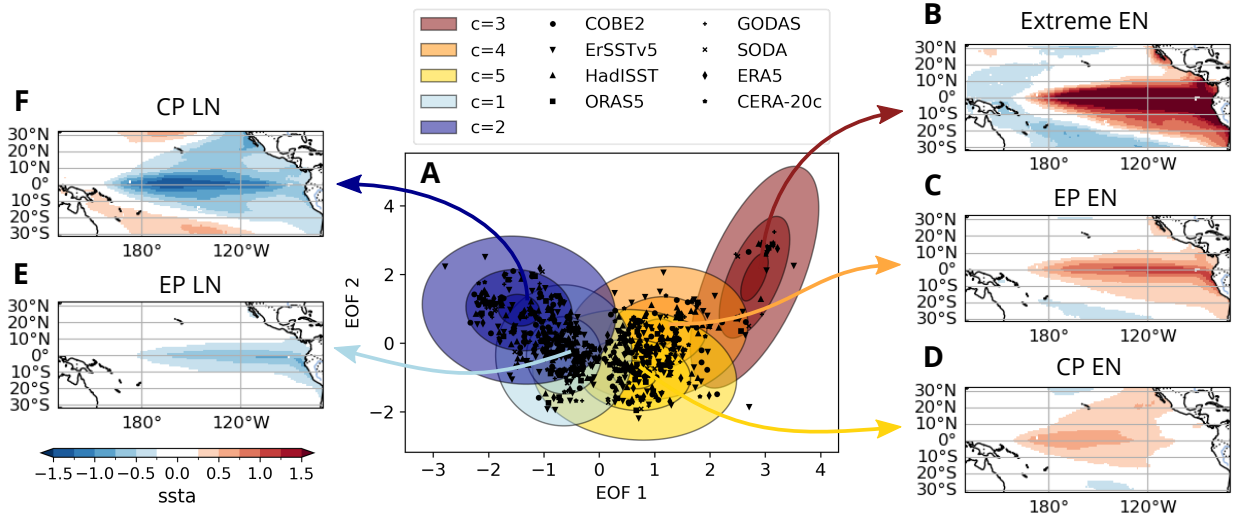


Figure 1: **El Niño and La Niña categories in PC1-PC2 space.** Monthly boreal winter (DJF) SSTAs of El Niño and La Niña events of all reanalysis products (see SI Tab. S1) projected onto the PC1-PC2 space and fitted by a Gaussian Mixture Model (GMM). Each event (DJF averages are shown as black dots in A) has a probability of belonging to each of the five categories (colored Gaussians in A). Pacific SSTA composites for each category are obtained by using the category membership as weights for the averages, depicted in panels (B-F). We obtain three El Niño-like patterns: *Extreme EN* (B), *Strong EN* (C), and *Weak EN* (D), while La Niña events form two categories: *Weak LN* (E) and *Strong LN* (F).

3 Results

3.1 ENSO diversity is well explained by five categories

The two most dominant EOFs of all eight SSTA datasets combined (Tab. S1) present the well-known spatial patterns associated with ENSO, i.e. EOF1 depicts the typical ENSO pattern with anomalies in the Central-Eastern Pacific, while EOF2 exhibits an east-west dipole structure (Fig. S2). Projection of the monthly SSTA of all boreal winter (December-January-February) El Niño and La Niña events onto EOF1 and EOF2, produces a distribution in the corresponding PC1–PC2 space that exhibits a wide, boomerang-like shape (Fig. 1A, Fig. S3). This nonlinear relationship between PC1 and PC2 has been considered an expression of key ENSO dynamics (Cai et al., 2018; Takahashi and Dewitte, 2016; Ham and Kug, 2012; Karamperidou et al., 2017), and used in the selection of models to consider for examining future projections (Cai et al., 2018, 2021). The nonlinear relationship itself can be accounted for by using a nonlinear transformation in place of the linear EOF-based transform, e.g., an autoencoder, and in that case, the boomerang-like shape is replaced by a simple linear relation between the two latent dimensions (SI Fig. S4 and SI Sec. S2).

The distribution of boreal winter El Niño and La Niña months in the PC1-PC2 space do not exhibit clear gaps visually, however, their density varies, suggesting a categorical structure (Takahashi and Dewitte, 2016). We model this distribution using a GMM with $k = 5$ categories (Eq. 1), a number determined using the BIC to ensure parsimony (see SI Sec. S3, Fig. S5A). The five Gaussians are arranged in a row along the boomerang-shaped distribution from the coldest events at the leftmost tip to the warmest events at the rightmost end (Fig. 1A).

We use the category memberships, $p(c_k|z(t))$, as weights for averaging the Pacific SSTAs of each category (SI Sec. S5) and find three El Niño-like patterns (Fig. 1B-D), and two La Niña-like patterns (Fig. 1E-F). Besides the different zonal locations of maximum warming/cooling, their defining factor is the tropical Pacific SSTA intensity. Hence, we will refer to the three El Niño categories as *Extreme EN* (Fig. 1B), *Strong EN* (Fig. 1C) and *Weak EN* (Fig. 1D), and correspondingly to *Weak LN* (Fig. 1E) and *Strong LN* (Fig. 1F) for the La Niña categories. We find that the overall clustering of the SSTA patterns into the five categories is robust (SI Sec. S6) upon changing the number of EOFs (SI Fig. S5B, Fig. S6, Fig. S7B), incorporating SSHA data along with the SSTA (SI Fig. S8 K-O), or varying the latitudinal range of the input (SI Fig. S8F-J). For comparison, we show the Gaussians for $k=4$ (SI Fig. S9), and $k=6$ (SI Fig. S10) categories.

The mean category membership for each boreal winter averaged across the datasets results in five time series of probabilities — one for each category — which reflect the likelihood of their occurrences (Fig. 2). We find that the indices are not sensitive to the dataset used for their estimation, as seen in the relatively small spread of the membership probabilities over the datasets at each time point (SI Fig. S11). As with the number of clusters, the category membership is also robust to changes in the number of variables, spatial domain, and the use of nonlinear encoding (SI Fig. S12).

Comparing the category membership series for *Strong* and *Weak EN* events (Fig. 2B, C) to two conventional classifications – the Niño3-Niño4 classification by Kug et al. (2009) and the EOF-based E/C classification by Takahashi et al. (2011) – we find that our classification mostly agrees with them (SI Tab. S2, Sec. S7). Differences, when they do occur, correspond to differences between the other classifications as well (Pascolini-Campbell et al., 2015; Yu and Kim, 2013; Capotondi et al., 2015). The two El Niños of 1994-95 and 2006-07, however, are classified by both conventional classifications as CP events, whereas we find them to be *Strong EN* events (Tab. S2). This is likely because the warm water anomalies span from the Central to the Eastern Pacific during the duration of these events, leading to possible ambiguities in the event definition (SI Fig. S13C, H). We also note that unlike the 1982-83 and 1997-98 events, which unambiguously belonged to the *Extreme EN* category, the 2015-16 event also has a nonzero membership in the *Strong EN* category, confirming its mixed nature.

3.2 Extreme EN events are different from Strong EN events

A key distinction of our ENSO categorization from conventional methods is the identification of the extreme El Niños as a separate class. While our *Weak EN* category corresponds to the conventional CP El Niño type, the conventional EP El Niño type is split into *Extreme EN* and *Strong EN* categories (SI Sec. S7, Tab. S2). SSTA composites of conventional EP El Niño events (SI Fig. S14A, C, E, Fig. S15B) exhibit the maximum warming in the eastern Pacific. The maximum warming is however strongly influenced by the few extreme EN events (1982/83, 1997/98, 2015/16), with an eastward shift of the peak towards the central Pacific when we exclude the extreme events (SI Fig. S14B, D, F).

The separation of *Extreme EN* from *Strong EN* events highlights differences in their impacts. We find that during *Extreme EN* events, statistically significant (at 95 % confidence) warmer-than-average SSTs and negative OLR anomalies occur in the Indian Oceans (SI Fig. S16A, K), which are not significant for *Strong EN* (SI Fig. S16B, L).

The two categories also differ in their evolution, analyzed using Hovmöller diagrams for the year preceding and succeeding an event (Fig. 3, SI Fig. S17). *Extreme EN* events show significant warm water volume anomalies, as described by SSHA, around the dateline already in the spring before an event, corresponding with a shift of the warm pool edge near the dateline (black line Fig. 3A, C). The *Extreme EN* onset phase also shows strong positive HF and LF

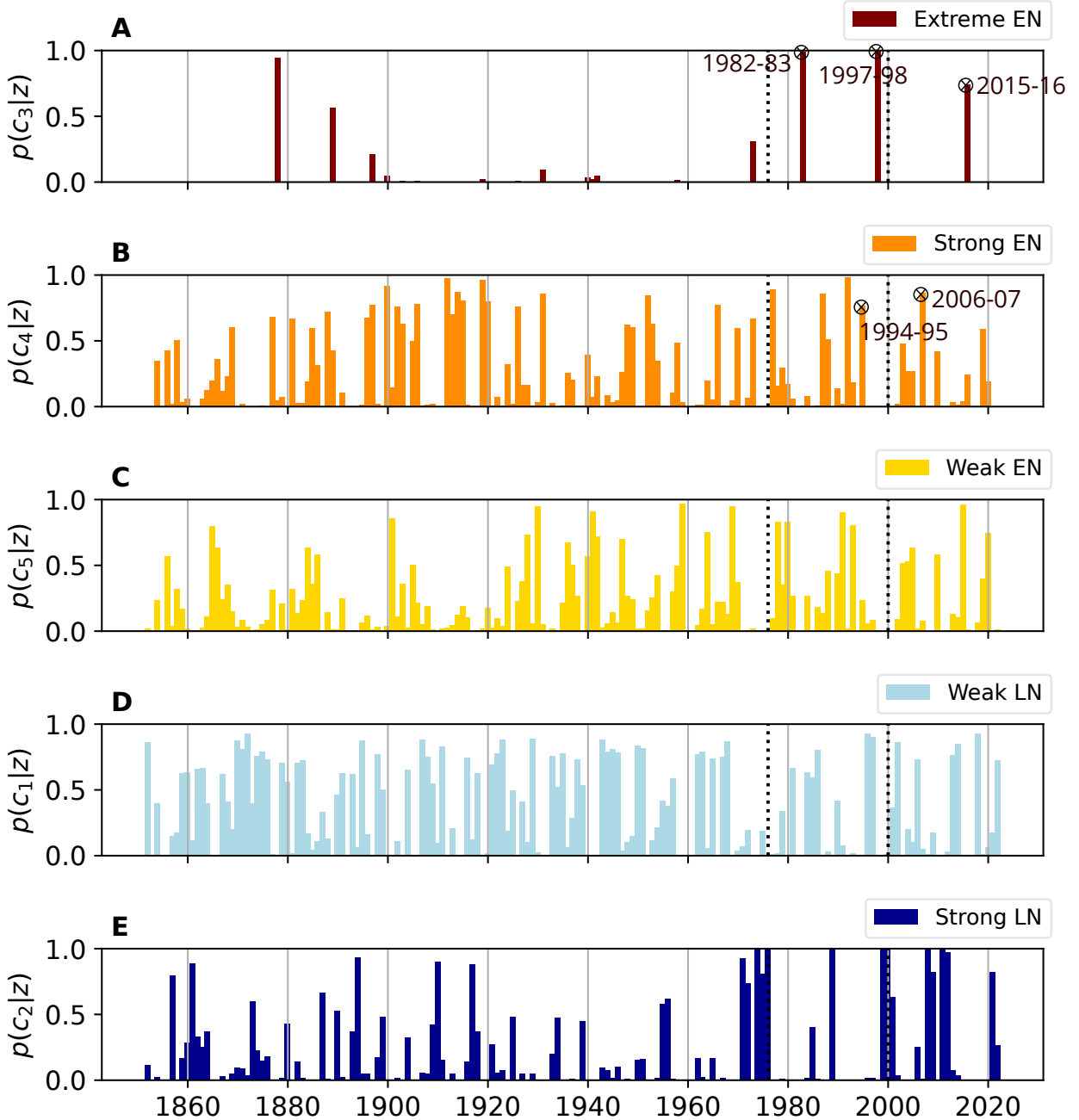


Figure 2: **Probabilistic category membership.** The GMM in Fig. 1 allows us to estimate the likelihood, $p(c_k|z(t))$, of each El Niño and La Niña winter month, $z(t)$, to belong to each of the categories, c_k (SI Sec. S4). An event belongs only to one category when its probability is 1. However, many events have shared probabilities across several categories. The categories are sorted in the following order (top to bottom): *Extreme EN* (A), *Strong EN* (B), *Weak EN* (C), *Weak LN* (D), and *Strong LN* (E). For visual reasons, we average the monthly probabilities over each winter (DJF) and over reanalysis products. The dashed lines indicate the reported shifts in ENSO variability in 1976-77 and 2000.

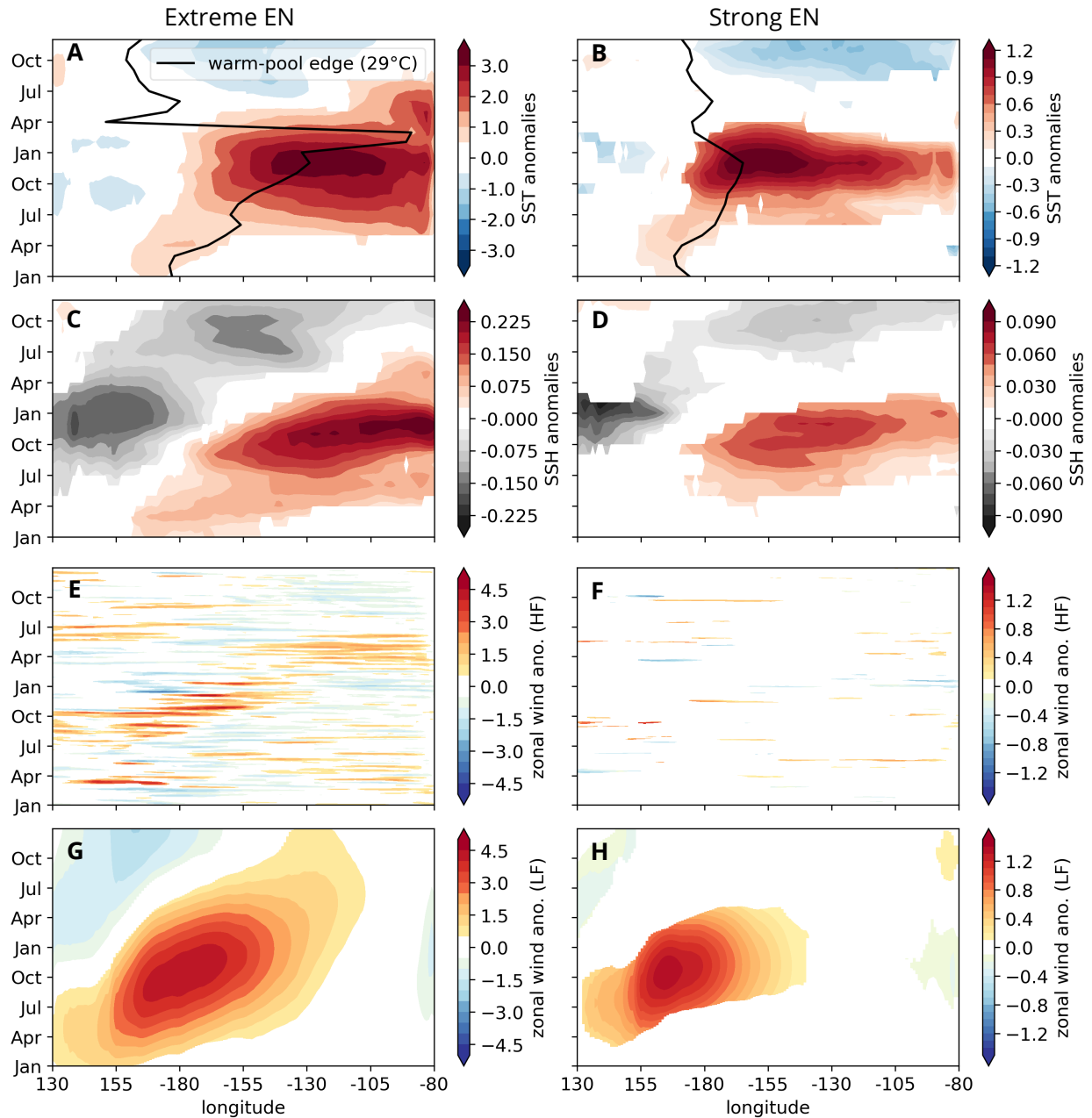


Figure 3: **Extreme EN and Strong EN category.** Hovmöller diagrams of SSTA (A, B), SSHA (C, D), high-frequency (HF) zonal wind anomalies (E, F), and low-frequency (LF) zonal wind (G, H) anomalies are obtained by meridional averages ($5^{\circ}\text{S} - 5^{\circ}\text{N}$) of each month in the year preceding and succeeding El Niño events. Each two-year period is weighted by the corresponding DJF average category membership probability (Fig. 2). The black line in (A) and (B) indicates the warm-pool edge, i.e., the 29°C SST isotherm (SI Sec. S8). Only values that are statistically significant above the 95th percentile are displayed (SI Sec. S9). SSTA and SSHA are taken from ORAS5 (1958–2022), while 10-meter zonal winds, with their HF- and LF components (Sec. S1) are computed from ERA5.

zonal wind components to the west of the dateline, during the preceding spring, extending further east as the event develops to its mature phase (Fig. 3E, G). *Strong EN* events, on the other hand, do not demonstrate a consistent onset pattern in the preceding spring (Fig. 3D, F, H).

These findings corroborate ideas presented in prior research on the impact of the Walker circulation’s zonal shift (Thual and Dewitte, 2023) and the influence of stochastic high-frequency winds, called Westerly Wind Bursts (WWBs), on ENSO Diversity (Fedorov et al., 2015; Capotondi et al., 2018; Puy et al., 2019).

3.3 Interdecadal ENSO variability is driven by Strong and Extreme events

The membership probabilities of each category (Fig. 2A, B) encode a distinct pattern of decadal-to-multidecadal ENSO variability. In particular, the *Strong LN* and the *Extreme EN* categories show a markedly prominent low-frequency variability, which is less evident in other categories. To quantify the low-frequency variation of ENSO, we multiply the Niño3.4 index (from HadISST) by the corresponding membership probabilities for each category (Eq. 2, Fig. 4A) and calculate their 20-year running variances every 10 years (Eq. 3). The variance of each category is normalized by the 20-year running variance of the Niño3.4 index (Fig. 4C) to determine their relative contributions.

The total variance of the Niño3.4 index shows a low-frequency modulation, with a minimum around 1920-1960, followed by an increasing trend, which is consistent with the shift in the mean and variance of ENSO after the so-called “1976-77 climate shift” (e.g., Miller 1994 (dashed line in Fig. 4C). A slight decrease in variance is noticeable after the year 2000, in line with the other reported climate shift (e.g., McPhaden 2012). While changes are noticeable in the variance of all categories, only minor contributions to the total Niño3.4 variance are observed for the *Weak LN* and *Weak EN* categories (Fig. 4D). The *Strong LN* category exhibits a substantial contribution starting around 1970, and the *Strong EN* category dominates the variance from 1890 to ~1930. Meanwhile, the contribution of the *Extreme EN* category is particularly visible towards the end of the 19th century and after 1980. These results are robust against variations in window size (SI Fig. S18) and using different reanalysis products (SI Fig. S19).

Between 20-40% of the decadal variance is due to the covariance between the different ENSO categories (denoted as *cov* in Fig. 4D). The covariance captures mainly the contribution of co-occurrences of different categories to the overall variance in a decade. However, other factors such as events with intermediate values of category memberships and statistical errors in estimating the GMM categories also influence the covariance. Our statistical approach does not allow us to assess the dynamics underpinning these decadal changes in the contribution of the different ENSO categories. ENSO decadal modulation is often associated with changes in the mean state, but it is not clear whether mean state changes are induced by influences from the extratropical Pacific or other ocean basins, or result as a residual of random variations of ENSO itself (Capotondi et al., 2023). Some studies, however, suggest that some ENSO events could induce decadal phase transitions through either nonlinear dynamical heating (Liu et al., 2022) or by inducing a discharge of upper ocean heat content in the off-equatorial Western Pacific (Meehl et al., 2021).

Our results provide novel insights into low-frequency changes in ENSO variance, which combines changes in frequency and intensity. We find that although the magnitude of total variance contributed by Eastern Pacific warming events (i.e. *Extreme EN* and *Strong EN events* combined) since the turn of the 20th century is comparable to that seen during the period from the 1880s to 1940s, the variance in the recent decades has been dominated by the *Extreme EN* category, a result consistent with the statistically significant change in ENSO properties in the late 1970s (Capotondi and Sardeshmukh, 2017). This shift was associated with a weakening of the easterly trade winds and a zonal reduction of the equatorial thermocline slope, conditions favoring stronger El Niño events. Linked to the increased contributions from *Extreme EN events* is the concurrent increase in the contributions of *Strong LNs* since the 1970s (dark blue in Fig. 4D), manifested in very strong, multi-year events starting around 1970 (Fig. 4A). These results are consistent with a higher likelihood of stronger CP La Niñas following the heat discharge of strong El Niños, as exemplified by the 1998-99 La Niña event after the extreme 1997-98 El Niño (Cai et al., 2015; Geng et al., 2023). While the increasing contribution of *Extreme EN* and *Strong LN* to ENSO variance starting around 1970 aligns with results from climate model simulations (Cai et al., 2021; Gan et al., 2023), our findings more specifically highlight the key role played by *Strong LN* in the ENSO variance changes after 1970.

We also find that during the ‘quiescent’ period of ENSO, roughly from the 1930s to the 1960s, most of the ENSO variability originated from Central Pacific warming and Eastern Pacific cooling events, i.e., from the weaker event types, while the influence of Central Pacific warming on the ENSO variance in recent decades has been almost negligible. This latter result is in apparent disagreement with the reported increase in intensity and frequency of CP events since 1980 (Lee and McPhaden, 2010), and especially after 2000 (dashed line in Fig. 4D; (McPhaden et al., 2011)). This discrepancy may be related to the 20-year running variance we used to construct Fig. 4D, and our inclusion of the 2015/16 El Niño, an event that was missing in the records used by the earlier studies.

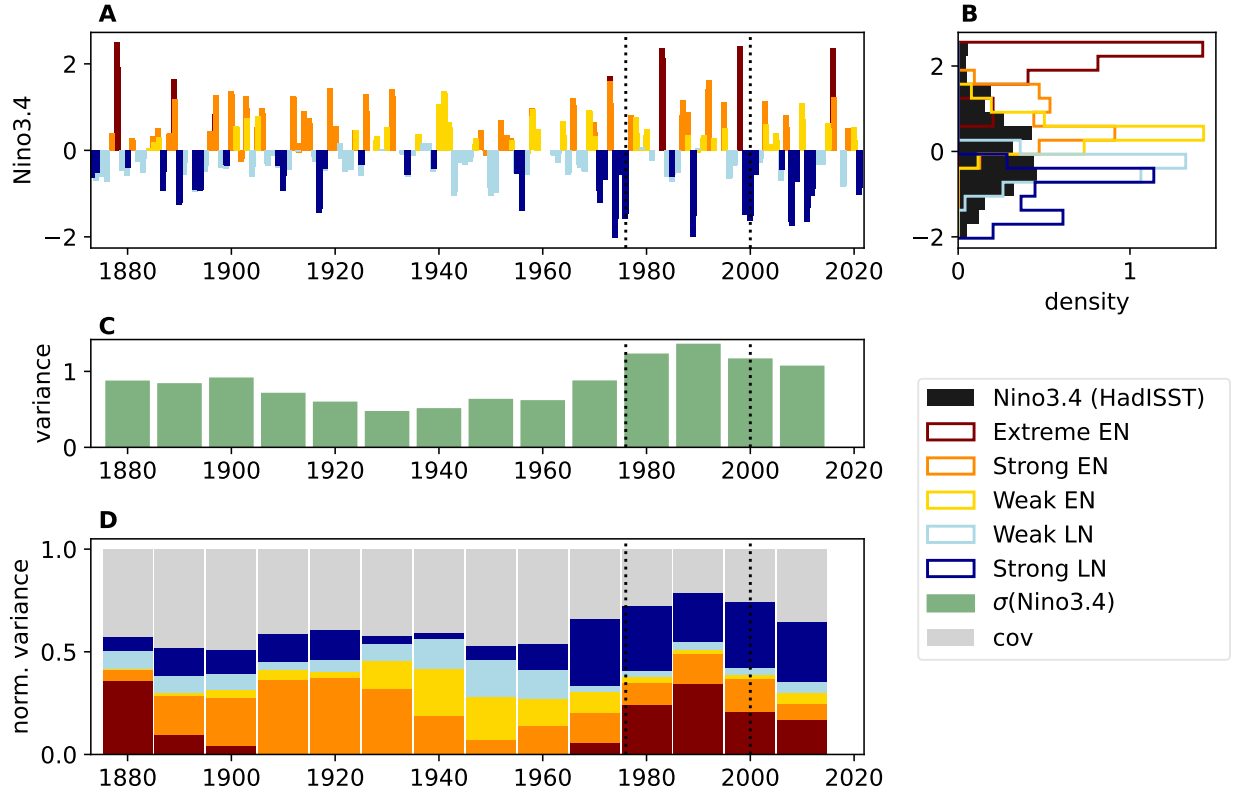


Figure 4: **Low-frequency changes of ENSO variance.** For each category, the Niño3.4 index is multiplied by their category membership probabilities (A). The histogram of Niño3.4 intensities (B), highlights different SSTA amplitudes between categories. The 20-year running variance of Niño3.4 every 10 years (C), is used to normalize the 20-year running variance of each category (D). *Extreme EN* and *Strong EN* categories dominate the Niño3.4 variance in the early and late 20th century. The variance shift in 1976-77 and 2000 (dashed lines) highlight reported changes in ENSO variability. The Niño3.4 index is taken from HadISST (Rayner et al., 2003).

4 Discussion

We present a new approach for studying the influence of ENSO diversity on low-frequency changes in ENSO variance. In particular, we use a Gaussian Mixture Model (GMM) within the low-dimensional PC1-PC2 space of monthly SSTA, which enables the assignment of non-binary event category memberships. We identify two La Niña categories (*Weak LN*, *Strong LN*) and three El Niño categories (*Extreme EN*, *Strong EN*, *Weak EN*), which combine the two dimensions of ENSO diversity — longitudinal location of maximum SSTA and its intensity. A key contribution of our work involves utilizing the membership probabilities to determine how each of the five categories individually affects the overall decadal variability in the Niño3.4 region. We find that the increasing frequency of both *Extreme EN* and *Strong LN* are the primary drivers of the increased ENSO variance post-1970. While these findings are consistent with previous studies that also detected an increase in extreme ENSO events in the second half of the 20th century (Cai et al., 2018, 2023), our results further highlight the key role played by the increasing frequency of *Strong LN* in these ENSO variance changes.

The proposed fuzzy clustering approach could also be used to quantify how well climate models represent ENSO diversity, akin to Dieppois et al. (2021) and Ayar et al. (2023). A preliminary analysis of the Community Earth System Model version 2 (CESM2) shows that this model only exhibits four ENSO categories instead of five (SI Sec. S10, Fig. S20), a discrepancy which cannot be explained by the different number of samples or other technical choices. Specifically, the *Extreme EN* category is missing in the model. While ENSO in CESM2 has an amplitude larger than observed, modeled SSTAs tend to occur preferentially in the central equatorial Pacific, with a more limited range of ENSO spatial patterns (Capotondi et al., 2020b), a behavior that seems to align with the model’s inability to simulate extreme events in the eastern Pacific. In addition, the model appears to underestimate ENSO’s nonlinearities, as quantified by the quadratic fit coefficient, α , in PC1-PC2 space (Dommenget et al., 2013; Karamperidou et al., 2017; Cai et al., 2018), which is smaller in CESM2 compared to reanalysis (Fig. S21). An extensive examination of several climate

models using our methodology is beyond the scope of this paper. However, our analysis of CESM2 demonstrates the potential value of our approach for achieving a detailed assessment of ENSO diversity in climate models. Such an investigation, as well as the analysis of possible changes in ENSO types in future climate scenarios, will be considered in subsequent studies.

Open Research

The data on which this article is based are publicly available in Zhang et al. (2019); Hersbach et al. (2020); COBE (2006); Rayner et al. (2003); ORAS5 (2021); Giese and Ray (2011); Behringer et al. (1998); Laloyaux et al. (2018), with their details are listed in SI Tab. S1. Our code is publicly available under Schlör (2023) and <https://github.com/jakob-schloer/LatentGMM.git>.

Acknowledgments

The authors thank the International Max Planck Research School for Intelligent Systems (IMPRS-IS) for supporting J. Schlör and F. Strnad. Furthermore, we express our gratitude to the NOAA Physical Science Laboratory for making their resources available for this study. Funded by the Deutsche Forschungsgemeinschaft (DFG, German Research Foundation) under Germany's Excellence Strategy – EXC number 2064/1 – Project number 390727645. We acknowledge support from the Open Access Publication Fund of the University of Tübingen. A. Capotondi was supported by the NOAA Climate Program Office's Climate Variability and Predictability (CVP) and Modeling, Analysis, Predictions and Projections (MAPP) programs and by DOE Award No. DE-SC0023228.

References

- Michael J. McPhaden. Evolution of the 2002/03 El Niño. *Bull. Am. Meteorol. Soc.*, 85(5):677–696, May 2004. ISSN 0003-0007. doi:10.1175/BAMS-85-5-677.
- Antonietta Capotondi, Andrew T. Wittenberg, Matthew Newman, Emanuele Di Lorenzo, Jin Yi Yu, Pascale Braconnot, Julia Cole, Boris Dewitte, Benjamin Giese, Eric Guilyardi, Fei Fei Jin, Kristopher Karnauskas, Benjamin Kirtman, Tong Lee, Niklas Schneider, Yan Xue, and Sang Wook Yeh. Understanding ENSO diversity. *Bulletin of the American Meteorological Society*, 96(6):921–938, June 2015. ISSN 15200477. doi:10.1175/BAMS-D-13-00117.1.
- Jong Seong Kug, Fei Fei Jin, and Soon Il An. Two types of El Niño events: Cold tongue El Niño and warm pool El Niño. *Journal of Climate*, 22(6):1499–1515, 2009. ISSN 08948755. doi:10.1175/2008JCLI2624.1.
- Antonietta Capotondi. ENSO diversity in the NCAR CCSM4 climate model: ENSO Diversity in the NCAR CCSM4. *Journal of Geophysical Research: Oceans*, 118(10):4755–4770, October 2013. ISSN 21699275. doi:10.1002/jgrc.20335.
- Felix M. Strnad, Jakob Schlör, Christian Fröhlich, and Bedartha Goswami. Teleconnection Patterns of Different El Niño Types Revealed by Climate Network Curvature. *Geophysical Research Letters*, 49(17):e2022GL098571, 2022. ISSN 1944-8007. doi:10.1029/2022GL098571.
- Margot Beniche. A distinct and reproducible teleconnection pattern over North America during extreme El Niño events. <https://www.researchsquare.com>, October 2023.
- Guomin Wang and Harry H. Hendon. Sensitivity of Australian Rainfall to Inter-El Niño Variations. *Journal of Climate*, 20(16):4211–4226, August 2007. ISSN 0894-8755, 1520-0442. doi:10.1175/JCLI4228.1.
- Hsun Ying Kao and Jin Yi Yu. Contrasting Eastern-Pacific and Central-Pacific types of ENSO. *Journal of Climate*, 22(3):615–632, February 2009. ISSN 08948755. doi:10.1175/2008JCLI2309.1.
- Regina R. Rodrigues, Reindert J. Haarsma, Edmo J. D. Campos, and Tércio Ambrizzi. The Impacts of Inter-El Niño Variability on the Tropical Atlantic and Northeast Brazil Climate. *Journal of Climate*, 24(13):3402–3422, July 2011. ISSN 0894-8755, 1520-0442. doi:10.1175/2011JCLI3983.1.
- Antonietta Capotondi, Shayne McGregor, Michael J. McPhaden, Sophie Cravatte, Neil J. Holbrook, Yukiko Imada, Sara C. Sanchez, Janet Sprintall, Malte F. Stuecker, Caroline C. Ummenhofer, Mathias Zeller, Riccardo Farneti, Giorgio Graffino, Shijian Hu, Kristopher B. Karnauskas, Yu Kosaka, Fred Kucharski, Michael Mayer, Bo Qiu, Agus Santoso, Andréa S. Taschetto, Fan Wang, Xuebin Zhang, Ryan M. Holmes, Jing-Jia Luo, Nicola Maher, Cristian Martinez-Villalobos, Gerald A. Meehl, Rajashree Naha, Niklas Schneider, Samantha Stevenson, Arnold Sullivan, Peter van Rensch, and Tongtong Xu. Mechanisms of tropical Pacific decadal variability. *Nature Reviews Earth & Environment*, 4(11):754–769, November 2023. ISSN 2662-138X. doi:10.1038/s43017-023-00486-x.
- Arthur J. Miller, Daniel R. Cayan, Tim P. Barnett, Nicholas E. Graham, and Josef M. Oberhuber. The 1976-77 Climate Shift of the Pacific Ocean. *Oceanography*, 7(1):21–26, 1994. ISSN 1042-8275.
- Michael J. McPhaden. A 21st century shift in the relationship between ENSO SST and warm water volume anomalies. *Geophys. Res. Lett.*, 39(9), May 2012. ISSN 0094-8276. doi:10.1029/2012GL051826.
- Pamela R. Grothe, Kim M. Cobb, Giovanni Liguori, Emanuele Di Lorenzo, Antonietta Capotondi, Yanbin Lu, Hai Cheng, R. Lawrence Edwards, John R. Southon, Guaciara M. Santos, Daniel M. Deocampo, Jean Lynch-Stieglitz, Tianran Chen, Hussein R. Sayani, Diane M. Thompson, Jessica L. Conroy, Andrea L. Moore, Kayla Townsend, Melat Hagos, Gemma O’Connor, and Lauren T. Toth. Enhanced El Niño–Southern Oscillation Variability in Recent Decades. *Geophysical Research Letters*, 47(7):e2019GL083906, 2020. ISSN 1944-8007. doi:10.1029/2019GL083906.
- Wenju Cai, Benjamin Ng, Tao Geng, Fan Jia, Lixin Wu, Guojian Wang, Yu Liu, Bolan Gan, Kai Yang, Agus Santoso, Xiaopei Lin, Ziguang Li, Yi Liu, Yun Yang, Fei-Fei Jin, Mat Collins, and Michael J. McPhaden. Anthropogenic impacts on twentieth-century ENSO variability changes. *Nature Reviews Earth & Environment*, 4(6):407–418, June 2023. ISSN 2662-138X. doi:10.1038/s43017-023-00427-8.
- Bastien Dieppois, Antonietta Capotondi, Benjamin Pohl, Kwok Pan Chun, Paul-Arthur Monerie, and Jonathan Eden. ENSO diversity shows robust decadal variations that must be captured for accurate future projections. *Communications Earth & Environment*, 2(1):212, October 2021. ISSN 2662-4435. doi:10.1038/s43247-021-00285-6.
- Jiale Lou, Matthew Newman, and Andrew Hoell. Multi-decadal variation of ENSO forecast skill since the late 1800s. *npj Climate and Atmospheric Science*, 6(1):1–14, July 2023. ISSN 2397-3722. doi:10.1038/s41612-023-00417-z.
- Allison E. Lawman, Pedro N. Di Nezio, Judson W. Partin, Sylvia G. Dee, Kaustubh Thirumalai, and Terrence M. Quinn. Unraveling forced responses of extreme El Niño variability over the Holocene. *Science Advances*, 8(9):eabm4313, March 2022. doi:10.1126/sciadv.abm4313.

- Wenju Cai, Agus Santoso, Matthew Collins, Boris Dewitte, Christina Karamperidou, Jong-Seong Kug, Matthieu Lengaigne, Michael J. McPhaden, Malte F. Stuecker, Andréa S. Taschetto, Axel Timmermann, Lixin Wu, Sang-Wook Yeh, Guojian Wang, Benjamin Ng, Fan Jia, Yun Yang, Jun Ying, Xiao-Tong Zheng, Tobias Bayr, Josephine R. Brown, Antonietta Capotondi, Kim M. Cobb, Bolan Gan, Tao Geng, Yoo-Geun Ham, Fei-Fei Jin, Hyun-Su Jo, Xichen Li, Xiaopei Lin, Shayne McGregor, Jae-Heung Park, Karl Stein, Kai Yang, Li Zhang, and Wenxiu Zhong. Changing El Niño–Southern Oscillation in a warming climate. *Nature Reviews Earth & Environment*, 2(9):628–644, September 2021. ISSN 2662-138X. doi:10.1038/s43017-021-00199-z.
- M. Pascolini-Campbell, D. Zanchettin, O. Bothe, C. Timmreck, D. Matei, J. H. Jungclaus, and H. F. Graf. Toward a record of Central Pacific El Niño events since 1880. *Theoretical and Applied Climatology*, 119(1-2):379–389, January 2015. ISSN 14344483. doi:10.1007/s00704-014-1114-2.
- Jin-Yi Yu and Seon Tae Kim. Identifying the types of major El Niño events since 1870. *International Journal of Climatology*, 33(8):2105–2112, June 2013. ISSN 08998418. doi:10.1002/joc.3575.
- Antonietta Capotondi, Andrew T. Wittenberg, Jong-Seong Kug, Ken Takahashi, and Michael J. McPhaden. ENSO Diversity. In *El Niño Southern Oscillation in a Changing Climate*, chapter 4, pages 65–86. American Geophysical Union (AGU), 2020a. ISBN 978-1-119-54816-4. doi:10.1002/9781119548164.ch4.
- Isma Abdelkader Di Carlo, Pascale Braconnot, Matthieu Carré, Mary Elliot, and Olivier Marti. Different Methods in Assessing El Niño Flavors Lead to Opposite Results. *Geophysical Research Letters*, 50(15):e2023GL104558, 2023. ISSN 1944-8007. doi:10.1029/2023GL104558.
- Karumuri Ashok, Swadhin K. Behera, Suryachandra A. Rao, Hengyi Weng, and Toshio Yamagata. El Niño Modoki and its possible teleconnection. *Journal of Geophysical Research: Oceans*, 112(11):C11007, November 2007. ISSN 21699291. doi:10.1029/2006JC003798.
- K. Takahashi, A. Montecinos, K. Goubanova, and B. Dewitte. ENSO regimes: Reinterpreting the canonical and Modoki El Niño. *Geophysical Research Letters*, 38(10):L10704, May 2011. ISSN 00948276. doi:10.1029/2011GL047364.
- Ken Takahashi and Boris Dewitte. Strong and moderate nonlinear El Niño regimes. *Climate Dynamics*, 46(5-6):1627–1645, March 2016. ISSN 14320894. doi:10.1007/s00382-015-2665-3.
- Wenju Cai, Guojian Wang, Boris Dewitte, Lixin Wu, Agus Santoso, Ken Takahashi, Yun Yang, Aude Carréric, and Michael J. McPhaden. Increased variability of eastern Pacific El Niño under greenhouse warming. *Nature*, 564(7735):201–206, December 2018. ISSN 14764687. doi:10.1038/s41586-018-0776-9.
- Na-Yeon Shin, Jong-Seong Kug, F. S. McCormack, and Neil J. Holbrook. The Double-Peaked El Niño and Its Physical Processes. *Journal of Climate*, 34(4):1291–1303, February 2021. ISSN 0894-8755, 1520-0442. doi:10.1175/JCLI-D-20-0402.1.
- Agus Santoso, Michael J. Mcphaden, and Wenju Cai. The Defining Characteristics of ENSO Extremes and the Strong 2015/2016 El Niño. *Reviews of Geophysics*, 55(4):1079–1129, 2017. ISSN 1944-9208. doi:10.1002/2017RG000560.
- Houk Paek, Jin-Yi Yu, and Chengcheng Qian. Why were the 2015/2016 and 1997/1998 extreme El Niños different? *Geophysical Research Letters*, 44(4):1848–1856, 2017. ISSN 1944-8007. doi:10.1002/2016GL071515.
- Lance Parsons, Ehtesham Haque, and Huan Liu. Subspace clustering for high dimensional data: A review. *SIGKDD Explor. Newsl.*, 6(1):90–105, June 2004. ISSN 1931-0145. doi:10.1145/1007730.1007731.
- Gideon Schwarz. Estimating the Dimension of a Model. *The Annals of Statistics*, 6(2):461–464, March 1978. ISSN 0090-5364, 2168-8966. doi:10.1214/aos/1176344136.
- Yoo-Geun Ham and Jong-Seong Kug. How well do current climate models simulate two types of El Niño? *Climate Dynamics*, 39(1-2):383–398, July 2012. ISSN 0930-7575, 1432-0894. doi:10.1007/s00382-011-1157-3.
- Christina Karamperidou, Fei-Fei Jin, and Jessica L. Conroy. The importance of ENSO nonlinearities in tropical pacific response to external forcing. *Climate Dynamics*, 49(7):2695–2704, October 2017. ISSN 1432-0894. doi:10.1007/s00382-016-3475-y.
- Sulian Thual and Boris Dewitte. ENSO complexity controlled by zonal shifts in the Walker circulation. *Nature Geoscience*, 16(4):328–332, April 2023. ISSN 1752-0908. doi:10.1038/s41561-023-01154-x.
- Alexey V. Fedorov, Shineng Hu, Matthieu Lengaigne, and Eric Guilyardi. The impact of westerly wind bursts and ocean initial state on the development, and diversity of El Niño events. *Climate Dynamics*, 44(5):1381–1401, March 2015. ISSN 1432-0894. doi:10.1007/s00382-014-2126-4.
- Antonietta Capotondi, Prashant D. Sardeshmukh, and Lucrezia Ricciardulli. The Nature of the Stochastic Wind Forcing of ENSO. *Journal of Climate*, 31(19):8081–8099, October 2018. ISSN 0894-8755, 1520-0442. doi:10.1175/JCLI-D-17-0842.1.

- Martin Puy, Jérôme Vialard, Matthieu Lengaigne, Eric Guilyardi, Pedro N. DiNezio, Aurore Voldoire, Magdalena Balmaseda, Gurvan Madec, Christophe Menkes, and Michael J. McPhaden. Influence of Westerly Wind Events stochasticity on El Niño amplitude: The case of 2014 vs. 2015. *Climate Dynamics*, 52(12):7435–7454, June 2019. ISSN 1432-0894. doi:10.1007/s00382-017-3938-9.
- N. A. Rayner, D. E. Parker, E. B. Horton, C. K. Folland, L. V. Alexander, D. P. Rowell, E. C. Kent, and A. Kaplan. Global analyses of sea surface temperature, sea ice, and night marine air temperature since the late nineteenth century. *J. Geophys. Res. Atmos.*, 108(D14):4407, July 2003. ISSN 0148-0227. doi:10.1029/2002JD002670.
- Chao Liu, Wenjun Zhang, Fei-Fei Jin, Malte F. Stuecker, and Licheng Geng. Equatorial Origin of the Observed Tropical Pacific Quasi-Decadal Variability From ENSO Nonlinearity. *Geophysical Research Letters*, 49(10):e2022GL097903, 2022. ISSN 1944-8007. doi:10.1029/2022GL097903.
- Gerald A. Meehl, Haiyan Teng, Antonietta Capotondi, and Aixue Hu. The role of interannual ENSO events in decadal timescale transitions of the Interdecadal Pacific Oscillation. *Climate Dynamics*, 57(7):1933–1951, October 2021. ISSN 1432-0894. doi:10.1007/s00382-021-05784-y.
- Antonietta Capotondi and Prashant D. Sardeshmukh. Is El Niño really changing? *Geophysical Research Letters*, 44(16):8548–8556, August 2017. ISSN 19448007. doi:10.1002/2017GL074515.
- Wenju Cai, Guojian Wang, Agus Santoso, Michael J. McPhaden, Lixin Wu, Fei-Fei Jin, Axel Timmermann, Mat Collins, Gabriel Vecchi, Matthieu Lengaigne, Matthew H. England, Dietmar Dommenges, Ken Takahashi, and Eric Guilyardi. Increased frequency of extreme La Niña events under greenhouse warming. *Nature Climate Change*, 5(2):132–137, February 2015. ISSN 1758-6798. doi:10.1038/nclimate2492.
- Tao Geng, Fan Jia, Wenju Cai, Lixin Wu, Bolan Gan, Zhao Jing, Shujun Li, and Michael J. McPhaden. Increased occurrences of consecutive La Niña events under global warming. *Nature*, 619(7971):774–781, July 2023. ISSN 1476-4687. doi:10.1038/s41586-023-06236-9.
- Ruyu Gan, Qi Liu, Gang Huang, Kaiming Hu, and Xichen Li. Greenhouse warming and internal variability increase extreme and central Pacific El Niño frequency since 1980. *Nature Communications*, 14(1):394, December 2023. ISSN 20411723. doi:10.1038/s41467-023-36053-7.
- Tong Lee and Michael J. McPhaden. Increasing intensity of El Niño in the central-equatorial Pacific. *Geophysical Research Letters*, 37(14):L14603, July 2010. ISSN 00948276. doi:10.1029/2010GL044007.
- M. J. McPhaden, T. Lee, and D. McClurg. El Niño and its relationship to changing background conditions in the tropical Pacific Ocean. *Geophysical Research Letters*, 38(15), 2011. ISSN 1944-8007. doi:10.1029/2011GL048275.
- Pradeebane Vaittinada Ayar, David S. Battisti, Camille Li, Martin King, Mathieu Vrac, and Jerry Tjiputra. A Regime View of ENSO Flavors Through Clustering in CMIP6 Models. *Earth’s Future*, 11(11):e2022EF003460, 2023. ISSN 2328-4277. doi:10.1029/2022EF003460.
- A. Capotondi, C. Deser, A. S. Phillips, Y. Okumura, and S. M. Larson. ENSO and Pacific Decadal Variability in the Community Earth System Model Version 2. *Journal of Advances in Modeling Earth Systems*, 12(12):e2019MS002022, 2020b. ISSN 1942-2466. doi:10.1029/2019MS002022.
- Dietmar Dommenges, Tobias Bayr, and Claudia Frauen. Analysis of the non-linearity in the pattern and time evolution of El Niño southern oscillation. *Climate Dynamics*, 40(11):2825–2847, June 2013. ISSN 1432-0894. doi:10.1007/s00382-012-1475-0.
- H.-M. Zhang, B. Huang, J. H. Lawrimore, M. J. Menne, and T. M. Smith. NOAA Global Surface Temperature Dataset (NOAAGlobalTemp), Version 5.0, 2019.
- Hans Hersbach, Bill Bell, Paul Berrisford, Shoji Hirahara, Julien Nicolas, Carole Peubey, Raluca Radu, Dinand Schepers, Adrian Simmons, Cornel Soci, Saleh Abdalla, Xavier Abellan, Gianpaolo Balsamo, Peter Bechtold, Gionata Biavati, Jean Bidlot, Massimo Bonavita, Giovanna De Chiara, Per Dahlgren, Dick Dee, Michail Diamantakis, Rossana Dragani, Johannes Flemming, Richard Forbes, Manuel Fuentes, Alan Geer, Leo Haimberger, Sean Healy, Robin J. Hogan, Sarah Keeley, Patrick Laloyaux, Philippe Lopez, Cristina Lupu, Gabor Radnoti, Patricia de Rosnay, Iryna Rozum, Freja Vamborg, and Sebastien Villaume. The ERA5 global reanalysis. *Q. J. R. Meteorolog. Soc.*, 146(730):1999–2049, July 2020. ISSN 0035-9009. doi:10.1002/qj.3803.
- COBE. COBE Sea Surface Temperature: NOAA Physical Sciences Laboratory COBE Sea Surface Temperature. <https://psl.noaa.gov/data/gridded/data.cobe.html>, 2006.
- ORAS5. ORAS5 global ocean reanalysis monthly data from 1958 to present, 2021.
- Benjamin S. Giese and Sulagna Ray. El Niño variability in simple ocean data assimilation (SODA), 1871-2008. *Journal of Geophysical Research: Oceans*, 116(2):C02024, 2011. ISSN 21699291. doi:10.1029/2010JC006695.

- David W. Behringer, Ming Ji, and Ants Leetmaa. An Improved Coupled Model for ENSO Prediction and Implications for Ocean Initialization. Part I: The Ocean Data Assimilation System. *Mon. Weather Rev.*, 126(4):1013–1021, April 1998. ISSN 1520-0493. doi:10.1175/1520-0493(1998)126<1013:AICMFE>2.0.CO;2.
- Patrick Laloyaux, Eric de Boisseson, Magdalena Balmaseda, Jean-Raymond Bidlot, Stefan Broennimann, Roberto Buizza, Per Dalhgren, Dick Dee, Leopold Haimberger, Hans Hersbach, Yuki Kosaka, Matthew Martin, Paul Poli, Nick Rayner, Elke Rustemeier, and Dinand Schepers. CERA-20C: A Coupled Reanalysis of the Twentieth Century. *J. Adv. Model. Earth Syst.*, 10(5):1172–1195, May 2018. ISSN 1942-2466. doi:10.1029/2018MS001273.
- Jakob Schlör. LatentGMM: An unsupervised fuzzy clustering approach for ENSO. Zenodo, November 2023.